Turbulent Diffusion in Particulately Fluidized Beds of Particles

THOMAS J. HANRATTY, GEORGE LATINEN, and RICHARD H. WILHELM

Princeton University, Princeton, New Jersey

Measuring the spreading of a tracer dye from a point source yields information on diffusion in glass-sphere beds fluidized in water. Particulately fluidized beds, which are here formed, are well described by the statistical turbulence equations of Taylor. Mixing parameters—eddy diffusivity, scale, and intensity of turbulence—are established. Transition of these variables is traced from fixed beds through fluidized beds in different degrees of bed expansion.

Mixing characteristics of these "ideal" types of fluidization may provide a frame of reference for consideration of more complex systems.

A study of diffusion in the continuous phase of a particulately fluidized bed of particles is of interest for two reasons. Particulate fluidization is suggested to represent, among the various possible modes of fluidization behavior, the smoothest or most "ideal" type. Knowledge gained about mechanisms of mixing through diffusional studies in this kind of system therefore may provide a frame of reference for consideration of more complex types of fluidization, such as are encountered in fluid-powder technology. Particulately fluidized beds are of interest also because they furnish an experimental illustration of aspects of the statistical formulation of diffusion in a turbulent field, proposed by Taylor (*14*) in 1921.

In particulate fluidization, individual particles have random motion and appear to be uniformly dispersed. There is little correlation between the fluctuating motions of adjacent particles. A counterpart is suggested in the molecular motions of an ideal gas. Particulate fluidization is achieved in high-density fluids with small density difference between particle and fluid, as in glass beads suspended in a rising stream of water.

Turbulence theory has been applied to various physical arrangements, commonly with the assumptions of homogeneity, i.e., independence of the translation of reference coordinates and isotropy, or independence of the rotation of the coordinates. An important application has been to steady-state turbulence in the central portion of a tube or duct for which a relatively flat velocity profile may be assumed. The decay of turbulence produced by flow through a stationary grid also has been a major topic of theoretical and experimental investigation. The effect on lateral diffusion of the presence of a fixed bed of particles in a fluid stream has been reported (*2, 12*). A fluidized bed, in turn, may be considered a transition system between unpacked and packed ducts. This is an arrangement for generating steady-state, fluid-phase turbulence through the presence of randomly spaced and randomly moving particles. The particle-population density is capable of being varied between the limits of a packed bed and of a duct in which the fluid stream is devoid of particles.

This paper sets forth particulate fluidization as an example of a turbulent system and establishes parameters such as eddy diffusivity, scale, and intensity of turbulence. The paper is based upon studies (*5, 12*) which may be consulted for details beyond those here presented.

*T. J. Hanratty is at present at the University of Illinois, Urbana, Illinois, and George Latinen with Monsanto Chemical Company, Springfield, Massachusetts.

THEORY

A turbulent field usually is considered to be a distribution of eddies ranging in size from dimensions that are too small to be measured to the dimensions of the container. Eddies are continually forming and disappearing within the field. Hence there exists a random motion of large masses of material, which is responsible for turbulent diffusion. Large-scale mixing results from the movement of larger eddies, whereas the small eddies are responsible for fine-grained mixing. This paper is concerned with averaged properties resulting from gross mixing.

It is instructive to compare molecular- and turbulent-diffusional processes between which two elements of dissimilarity have been noted. In molecular diffusion, experimental distances are large compared with the molecular mean free path. In turbulent diffusion such simplification may not be counted on. Experimental measurements can well be made within a turbulent "mean free path" or scale. As a result, for diffusion from a fixed-point source, the size of the turbulent-diffusion coefficient ($\overline{X^2}/2t$) is found to depend upon the time of diffusion, reaching constancy only after a long time interval has elapsed in a given experiment. A second difference between molecular and turbulent diffusion relates to the elementary mechanism steps. The former may be represented as consisting of discrete motions of single particles. By contrast, turbulent diffusion must be thought to involve continuous variation of properties because masses of material move about and continuously change their identity. These elements of difference were recognized by Taylor (*14*) and were given quantitative expression in his equation for turbulent diffusion. Confirmation of Taylor's formulation rests upon a limited number of experimental investigations to date: behind a grid in a wind tunnel (*15, 18, 19*), in a circular duct (*16*), and in a channel (*8, 9*).

To serve in interpreting diffusion measurements in the continuous phase of a fluidized mass of particles, Taylor's equations and other pertinent theoretical background are summarized herewith.

A fixed-point source located at $x = 0$ in a homogeneous isotropic turbulent field is assumed.* Assumed also is the x component of motion of a diffusing particle of fluid. If the velocity component in this direction is u, the displacement of a single particle after a time t is

$$X = \int_0^t u\,dt \qquad (1)$$

Because of the random nature of turbulent motion a plus or minus value for X is equally probable. Therefore, averaged for a large number of particles, $\overline{X} = 0$. However, if the value X^2 be averaged, a finite value will result, $\overline{X^2} \neq 0$. $\overline{X^2}$ will be a measure of the spread which may be expected in a given diffusion time.

The quantity $\overline{X^2}$ may be expressed as a function of the diffusional dispersion time, t, the root-mean-square fluctuating-velocity component, $\overline{u^2}$, and a correlation coefficient,

$$R = \frac{\overline{u_{t_1}u_{t_2}}}{\overline{u^2}}.$$

The covariance $\overline{u_{t_1}u_{t_2}}$ represents the average for a large number of particles of the product of the velocity of a particle at time t_1 and its velocity after a time, $s = t_2 - t_1$. For very large values of s there is no correlation between u_{t_1} and u_{t_2}; i.e., the product can be plus as often as minus $\overline{u_{t_1}u_{t_2}} = 0$. For the case of a small s, the motion of the particle at time t_1 will resemble motion at t_2. If u_{t_1} is negative, then it is probable that u_{t_2} will be negative. Likewise if u_{t_1} is positive, it is probable that u_{t_2} will be positive. Therefore, it is likely that $u_{t_1} \cdot u_{t_2}$ will be positive for a large number of particles; $\overline{u_{t_1}u_{t_2}}$ = positive value.

G. I. Taylor was the first to use these concepts to describe diffusion from a fixed-point source in a homogeneous isotropic field. Kampe de Feriet (*4, 10*) has also considered this problem, and the

*In the present work diffusion measurements were performed only in two dimensions and generally under such conditions that diffusion in the third dimension may be neglected. Present work has therefore been proved to be isotropic in two dimensions. Isotropy in three dimensions is assumed in the present development.

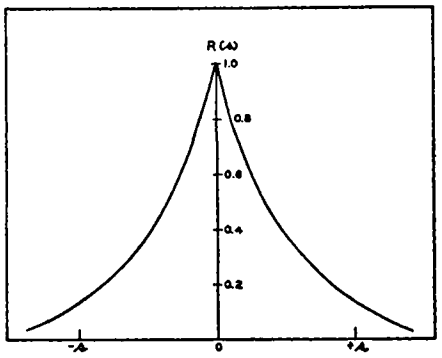

Fig. 1. Typical form of Taylor-de Feriet correlation $R(s)$ for turbulent-velocity fluctuations at time intervals, s.

expression for $\overline{X^2}$, derived by the latter author, is presented below:

$$\overline{X^2} = \int_0^t \int_0^t \overline{u_{t_1} u_{t_2}}\, dt_1\, dt_2$$

$$\overline{u_{t_1} u_{t_2}} = \overline{u^2} R(t_2, t_1)$$

If the field is steady, i.e., $\overline{u_{t_1} u_{t_2}}$ is a function only of $t_2 - t_1$ and not of t_2 or t_1, then

$$\overline{u_{t_1} u_{t_2}} = \overline{u^2} R(t_2 - t_1) = \overline{u^2} R(s)$$

$$\overline{X^2} = \int_0^t \int_0^t \overline{u^2} R(s)\, dt_1\, dt_2$$

Since $R(s)$ is an even function,

$$\overline{X^2} = 2 \int_0^t (t - s) \overline{u^2} R(s)\, ds \quad (2)$$

Because of the nature of the turbulent field, $R(s)$ will vary continuously from 1 to 0 as s varies from 0 to ∞ in a form similar to that shown in Figure 1. The $\overline{X^2}$ vs. t curve has a form depicted in Figure 2. The behavior of the Taylor-de Feriet equation in the limits may be obtained by integration. For t very small, $t \to 0$, $R_s \to 1$:

$$\overline{X^2} = 2\overline{u^2} \int_0^t (t - s)\, ds = \overline{u^2} t^2; \quad (3)$$

$$\sqrt{\overline{X^2}} = \sqrt{\overline{u^2}}\, t$$

For t very large:

$$\overline{X^2} = 2\overline{u^2} \int_0^t tR(s)\, ds - 2\overline{u^2} \int_0^t sR(s)\, ds \quad (4)$$

$$\int_0^t R(s)\, ds \to \text{const.} = \tau = \int_0^\infty R(s)\, ds$$

$$\int_5^t sR(s)\, ds \to \text{const.} = \int_0^\infty sR(s)\, ds$$

since $R(s)$ approaches zero in an exponential manner for large t,

$$\overline{X^2} = 2\overline{u^2}\tau t - 2\overline{u^2}(\text{const.}) \quad (5)$$

For the calculation of the root-mean-square displacement $\overline{X^2}$ at intermediate times, the dependence of R upon the time interval s must be known. It is convenient to assume the exponential relation

$$R(s) = e^{-s/\tau} \quad (6)$$

in which τ is a constant which is a property of the field and may be looked upon as the average lifetime of eddies responsible for diffusion. Turbulent-diffusion studies by Kalinske and Pien (*9*) are satisfactorily approximated by this relation, as are also the results of the present work.

The integrals in Equation (4) may now be evaluated as follows:

$$\int_0^\infty R(s)\, ds = \int_0^\infty e^{-s/\tau}\, ds = \tau \quad (7)$$

$$\int_0^\infty sR(s)\, ds = \int_0^\infty se^{-s/\tau}\, ds = \tau^2 \quad (8)$$

Equation (4) thus becomes

$$\overline{X^2} = 2\overline{u^2}\tau t - 2\overline{u^2}\tau^2 \quad (9)$$

As shown in Figure 2, the intercept of this relation on the t axis occurs at $t = \tau$.

Employing Equation (6) one may write a general expression for $\overline{X^2}$:

$$\overline{X^2} = 2\overline{u^2}\tau^2 \left[\frac{t}{T} - (1 - e^{-t/\tau})\right] \quad (10)$$

Therefore $\overline{X^2}/2\overline{u^2}\tau^2$ is a unique function of t/τ. Kalinske and Pien (*9*) correlated diffusion data by means of these variables.

HOMOGENEOUS ISOTROPIC SYSTEMS INVOLVING TURBULENT DIFFUSION

The variation of $\overline{X^2}$ with time for molecular diffusion from a fixed point has been shown by Einstein (*3*) to be

$$\frac{\overline{X^2}}{2t} = D = \text{constant} \quad (11)$$

where D = molecular diffusivity. Systems involving molecular diffusion may be described by the Fick's law differential equation using appropriate boundary conditions:

$$\frac{\partial c}{\partial t} = \nabla \cdot (D \nabla C) \quad (12)$$

The use of this equation implicitly involves the assumption that the diffusion characteristics of particles contained in a differential volume are independent of their previous history, i.e., the length of time they have been in the field. This independence is not encountered in turbulent diffusion, i.e., $\overline{X^2}/2t$ is a function of time. Therefore Fick's law may not be used to describe the diffusion of particles which have been in the field for different lengths of time. The description of turbulent systems must be accomplished by defining the diffusion behavior of a single source or sink of heat or mass and then representing the system as consisting of a number of distributed sources and sinks.

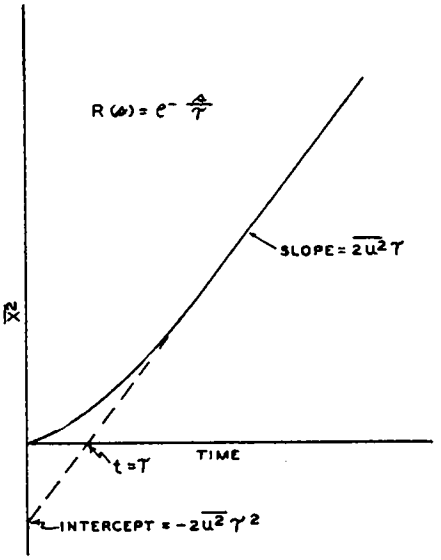

Fig. 2. Relation between $\overline{X^2}$ for diffusion from a point source with time when the correlation for turbulent-velocity fluctuations is approximated by $R(s) = e^{-s/\tau}$

Batchelor (*1*) and Hanratty (*6*) have shown that Equation (12) with a diffusion coefficient which varies with time can be used to describe the behavior of a single instantaneous source or sink

$$\frac{\partial C}{\partial t} = \phi(t) \nabla^2 C \quad (13)$$

provided that (1) the diffusion coefficient be defined as

$$\phi(t) = \frac{1}{2} \frac{d\overline{X^2}}{dt} \quad (14)$$

and (2) the distribution describing $\overline{X^2}$ be Gaussian:

$$P\, dx\, dy\, dz = \frac{1}{(2\pi\overline{X^2})^{3/2}} \cdot \exp\left[-\frac{x^2 + y^2 + z^2}{2\overline{X^2}}\right] dx\, dy\, dz \quad (15)$$

$P\, dx\, dy\, dz$ = probability of finding a particle between x and $x + dx$, y and $y + dy$, z and $z + dz$.

For the description of the experiments described in this paper it is convenient to consider the solution to Equation (13) for a cylindrical polar-coordinate system for radial symmetry for the case in which diffusion in the z direction is important and also for the case in which it is negligible. The equations to be solved are then as follows:

$$\frac{\partial C}{\partial t} = \phi(t)\left[\frac{\partial^2 C}{\partial r^2} + \frac{1}{r}\frac{\partial C}{\partial r} + \frac{\partial^2 C}{\partial z^2}\right] \quad (16)$$

$$\frac{\partial C}{\partial t} = \phi(t)\left[\frac{\partial^2 C}{\partial r^2} + \frac{1}{r}\frac{\partial C}{\partial r}\right] \quad (17)$$

If N units of material, or N units per unit length for the two-dimensional case, emitted into the field at zero time from a position $r = 0$, $z = 0$, are considered, the solutions of Equations (16) and (17) for boundary conditions

$$t > 0$$

$$C \to 0 \quad \text{as} \quad r \to \infty$$

$$C \to 0 \quad \text{as} \quad z \to \infty$$

are respectively longitudinal diffusion important:

$$C = \frac{N}{(2\pi)^{3/2}[\int_0^t 2\phi\, dt]^{3/2}} \cdot \exp\left\{-\frac{r^2 + z^2}{2\int_0^t 2\phi\, dt}\right\} \quad (18)$$

negligible longitudinal diffusion:

$$C = \frac{N}{(2\pi)[\int_0^t 2\phi\, dt]} \exp\left\{-\frac{r^2}{2\int_0^t 2\phi\, dt}\right\} \quad (19)$$

When the diffusing time is long enough so that material reaches the container walls, the boundary conditions become for $t > 0$

$$z = +\infty \qquad C = C_A$$

$$z = -\infty \qquad C = 0$$

$$r = a \qquad \frac{\partial C}{\partial r} = 0$$

The solutions of Equations (16) and (17) are then longitudinal diffusion important:

$$C = \frac{N \exp\left\{-\frac{z^2}{4\int_0^t \phi\, dt}\right\}}{\pi a^2 \sqrt{2\pi}\,[\int_0^t 2\phi\, dt]^{1/2}} \cdot \sum_0^\infty \exp\left\{-\beta_n^2 \int_0^t \phi\, dt\right\} \frac{J_0(\beta_n r)}{J_0^2(\beta_n a)} \quad (20)$$

longitudinal diffusion unimportant:

$$C = \frac{N}{\pi a^2} \sum_0^\infty \exp\left\{-\beta_n^2 \int_0^t \phi\, dt\right\} \cdot \frac{J_0(r\beta_n)}{J_0^2(a\beta_n)} \quad (21)$$

where β_n is defined by the equation below:

$$J_1(\beta_n a) = 0 \quad (23)$$

The validity of the preceding four solutions [Equations (18) to (21)] can be seen by substituting back into Equations (16) and (17). These solutions are identical with those that would be obtained by solving Equation (12) if it is assumed that D = constant if one substitutes in the final expression

$$Dt = \int_0^t \phi\, dt$$

Hence a turbulent diffusivity, E, analogous to D may be defined as

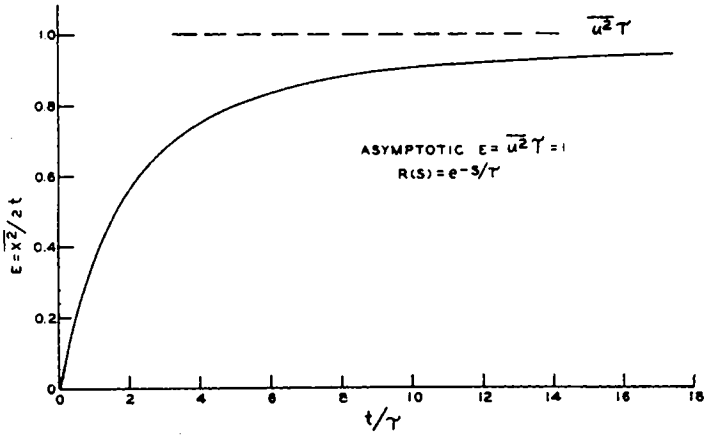

Fig. 3 Graph showing that eddy diffusivity varies with time of diffusion in a turbulent field and ultimately reaches a constant value.

$$E = \frac{1}{t}\int_0^t \phi\, dt = \frac{\overline{X^2}}{2t} \quad (24)$$

Unlike molecular diffusion from a fixed-point source, E will vary with time. If Equation (2) is used, an expression may be written for E for a homogeneous isotropic field:

$$E = \frac{\overline{X^2}}{2t}\int_0^t (t - s)R(s)\, ds$$

If Equation (6) is valid the foregoing expression may be integrated to yield

$$E = \overline{u^2}\tau\left[1 - \frac{\tau}{t}(e^{-t/\tau} - 1)\right] \quad (25)$$

This function is plotted in Figure 3. Only for large times of diffusion does E level out to a constant value.

TURBULENT FLOW SYSTEM INVOLVING DIFFUSION FROM A CONTINUOUS SOURCE

Theory presented up to this point has been for isotropic, homogeneous turbulence, conditions which at best can be only approximated. Flow in ducts, for example, may deviate from ideal conditions because of the effect of walls on the flow profile and on turbulence isotropy and homogeneity. Even if a uniform flow existed, the condition of isotropy might not be satisfied as diffusion in the direction of flow might be different from that in other directions. If turbulence is caused by a grid, there will be a continuous state of decay of the turbulence in the stream. The experimental system used in this research consisted of diffusion from a continuous source of material located in the center of a "particulate" fluid bed through which fluid is flowing in the z direction. The fluid velocity is substantially uniform in the cross section of the container, and, although there must necessarily be a decay of turbulence, continuous concurrent replenishment proceeds from the suspended particles. It has been assumed therefore that the field may be considered homogeneous and isotropic in the radial direction. Turbulence is probably not the same in the r as in the z direction.

The equations developed in the theory section may be used if the system is represented as a number of instantaneous sources which are carried downstream with the fluid. Each one of these sources will spread out equally in all directions and thus consists of a spherical cloud of the material which increases in radius as it is transported downstream. The case in which longitudinal diffusion is neglected is represented by a number of sources which spread out only in the radial direction and therefore is represented by a series of expanding disks.

At $r = 0$ and at a distance z' from the injection point is a source which has been in the field a time $t = z'/U$. The concentration profile in a cross section at a given value of z will result from contributions of sources that have been in the field for times ranging from 0 to ∞. When longitudinal diffusion is neglected, only a source which has been in the field a time $t = z/U$ will contribute to the concentration profile at a longitudinal distance z from the injector.

Equations (18) and (20) may be used to describe the contribution of a single source if the quantity $(Ut - z)$ is substituted for z. The sum of the effect of all the sources is obtained in the following manner:

wall effect unimportant:

$$C = \int_0^\infty \frac{Q\, dt}{[2\pi\int_0^t 2\phi\, dt]^{3/2}} \cdot \exp\left\{-\frac{r^2 + (Ut - z)^2}{4\int_0^t \phi\, dt}\right\} \quad (26)$$

wall effects important:

$$C = \int_0^\infty \frac{Q\, dt \exp\left\{-\frac{(Ut - z)^2}{4\int_0^t \phi\, dt}\right\}}{\pi a^2[2\pi\int_0^t 2\phi\, dt]^{1/2}} \cdot \sum_0^\infty \exp\left\{-\beta_n^2 \int_0^t \phi\, dt\right\} \frac{J_0(\beta_n r)}{J_0^2(\beta_n a)} \quad (27)$$

Q = rate of flow of material from the injector

Equations (19) and (21) may be used to describe a continuous source by substituting $t = z/U$.

wall effects unimportant:

$$C = \frac{N}{(2\pi)[\int_0^{t/U} 2\phi\, dt]} \cdot \exp\left\{-\frac{r^2}{2\int_0^{t/U} 2\phi\, dt}\right\} \quad (28)$$

wall effects important:

$$C = \frac{N}{\pi a^2} \sum_0^{\infty} \exp\left\{-\beta_n^2 \int_0^{t/U} \phi\, dt\right\} \cdot \frac{J_0(r\beta n)}{J_0^2(a\beta_n)} \quad (29)$$

Equation (28) is the Gaussian error curve.

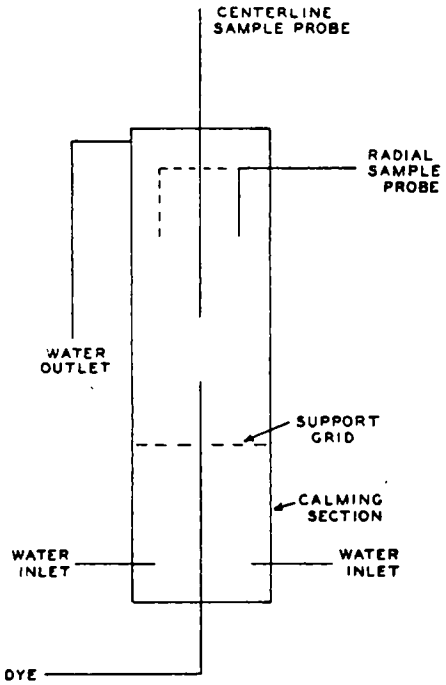

Fig. 4. Elements of apparatus for measuring diffusion of tracer from a point source into a fluidized bed.

EXPERIMENTAL

As noted above, turbulent diffusion may be characterized by two of the following parameters: an asymptotic value of E, an intensity $\sqrt{\overline{u^2}}/U$, and a scale factor τ. The measure of spread of a tracer material from a fixed-point source into the turbulent field (as determined in the present work) served as a convenient technique for finding these properties. The particulately fluidized bed here used consisted of uniformly sized spherical glass beads suspended in an upward stream of water flowing in a 5.4-cm. tube. The size of bead, 3 mm. in diameter, was carefully chosen to give a representative "ideal" system, i.e., one that is described by a Taylor $\overline{X^2}$ vs. t function. When glass beads of smaller size were employed, the scale of turbulence was found to be very small, leading to precision difficulties in measuring this relation. Larger glass spheres were not used because of possible wall effects with large particle-to-tube-diameter ratios. Heavier particles of lead 3-mm. spheres lead to "nonideal" behavior (*5*), in which the Taylor $\overline{X^2}$ function does not hold, a system which is not included in the present discussion.

Fluidized glass beads are in random motion which from observation appears to lack strong correlation in the motion of neighboring particles except for an over-all net movement up one side of the tube and down the other, an action which is slow compared with movements of individual particles relative to each other. Diffusion measurements were restricted to the central section of the tube, away from the upper and lower ends, at which there is lateral motion of particles.

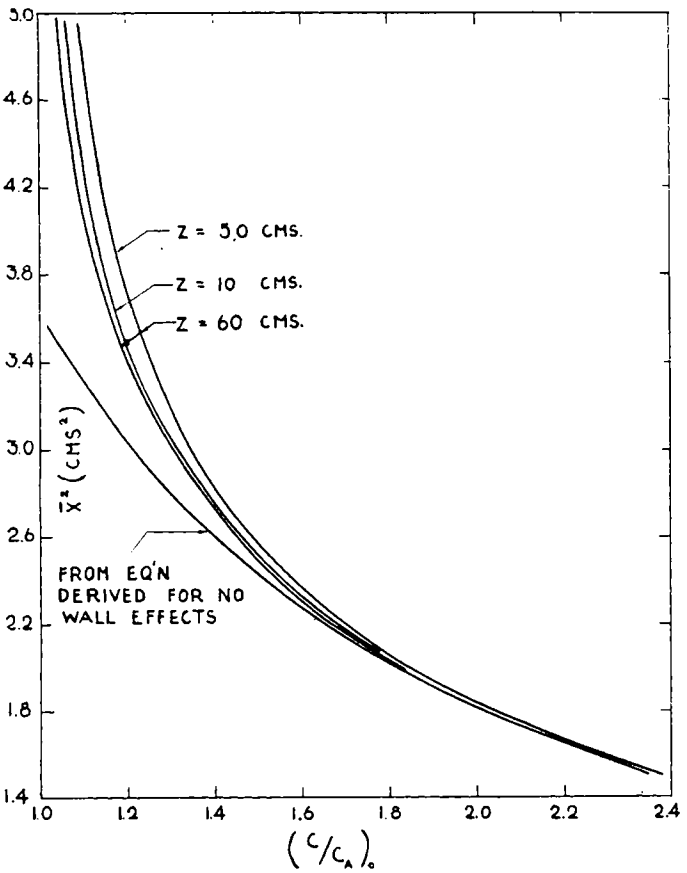

Fig. 5. Computed relationships between $\overline{X^2}$ and center-line compositions (C/C_A) at different coordinate distances between source and sampling taps. $\overline{X^2}$ is a measure of tracer spreading under the condition of $U_{AVG}/U = 1$ and the hypothetical condition of no containing walls and zero fluid velocity.

Apparatus

The equipment was substantially that used by Bernard and Wilhelm (*2*) and Latinen (*12*). A line sketch is shown in Figure 4. Features of the design are as follows:

The column was a Lucite tube 5.40 cm. I.D., 25.1 cm. long. Methylene blue dye, concentration 4 g./1,000 ml. of water, was admitted to the fluidized bed of particles from a centrally located stainless tube entering from the bottom. The tracer-tube position could be varied vertically from a position flush with the support plate to an elevation of 9.2 cm. from the plate. The tracer tube was 1/16 in. I.D., ⅛ in. O.D., and was tapered to 3/32 in. at the point of injection. Dye was introduced from a storage tank pressurized with nitrogen.

The main water stream was pumped to a distributor and thence through eight equally spaced radial arms to a turret at the base of the column. This design ensured a symmetrical feed to the column.

A calming section preceded the column proper to ensure a uniform-flow profile and to break up any large-scale eddies which might have formed. The calming section consisted of a 12 in. length of piping packed with 1-mm. glass spheres.

The support plate for the bed was a grid made by milling 0.020-in. grooves 0.020 in. apart into each face of a 1.6-in. brass disk. The two series of grooves were at right angles to one another so that the net effect was of a plate having uniformly sized and spaced 0.020-in. square holes. The plate was covered with a fine-mesh screen to prevent small particles from being jammed in the openings.

Water flow rates were measured by means of rotameters, and the tracer-dye flow rate was determined from the known water flow rate and the average concentration in the column effluent. The temperature of the water was measured.

Two types of sampling traverses were made, radial and center line. The radial sampling probe consisted of a horizontal leg of ⅛-in. stainless steel tubing which entered at a position about 10 cm. above the top level of the fluid bed. A length of similar tubing with a 2-in. piece of 3/64-in. hypodermic tubing soldered into the end constituted the vertical segment. By using probes having vertical legs of different length, one could vary the longitudinal position of the traverse.

The center-line probe consisted of a length of ⅛-in. stainless steel tubing which was tapered to an outside diameter of 3/32 in. at the sampling position. It entered through the top of the column and was held in a central position by three 1/16-in.-diam. brass rods which were soldered to the probe at a position 2¾ in. from its tip. A vernier was etched on the surface of the tubing so that its position might be determined directly.

Probe samples were analyzed with a Fisher electrophotometer having a red filter.

Procedure

Data may be obtained over a range of fluidized-bed properties depending on the flow rates, bed heights, and fractions void. In all runs except two, a constant bed height of 20.3 cm. was maintained. Fractions void and flow rates were varied by changing the amount of solids in the bed.

The operating procedure was as follows. After the lines were flushed, water was admitted to the column which contained a known weight of spheres. The bed was expanded to the standard height. After an initial flushing of lines, the dye rate was adjusted to a velocity slightly less than that of the surrounding water stream. Time-average tracer samples were secured by a slow, uniform withdrawal over a period ranging from 1½ to 2½ min. It was determined that sample compositions do not depend upon withdrawal rates at these low withdrawal velocities.

REDUCTION OF DATA

Two types of data were obtained: radial traverses in a plane at a fixed longitudinal distance from the plane of the source and center-line traverses. Radial traverses were measured to examine the validity of the equations developed in preceding sections of this paper and to obtain information about the nature of the distribution describing $\overline{X^2}$.

In order to evaluate the parameters intensity $\sqrt{\overline{u^2}/U}$ and scale τ, it is necessary to obtain the $\overline{X^2}$ vs. t relation that one of the single instantaneous sources would possess under the hypothetical condition of zero flow and no confining boundaries. Experimentally the relationship is conveniently obtained from the longitudinal traverse.

The experiments described in this paper were such that diffusion in the flow direction could not be measured. Therefore the equations developed for a two-dimensional source were used in examining the data. Throughout most of the field concentration gradients in the flow direction were much smaller than in the radial direction and the foregoing simplification was a valid one. However, close to the source this is not true and longitudinal diffusion will affect the measured concentration profiles.

The amount of material flowing from the injector per unit time may be calculated from the mixed average concentration of the column effluent, C_A, and the average velocity over the tube cross section within the fluidized bed.

$$Q = C_A \pi a^2 U_{AVG} \qquad (30)$$

The flux of diffusing material at any point in the tube is UC where U is the velocity of the fluid at that point. The quantity $UC/(\pi a^2 U_{AVG} C_A)(2\pi r\, dr)$ then represents the probability of finding a particle of the diffusing material in the differential area $2\pi r\, dr$. In terms of the nomenclature used in Equations (28) and (29) this is equal to $(C/N)2\pi r\, dr$.

These equations may be rewritten in the following form:

$$\frac{C}{C_A} = \left(\frac{U_{AVG}}{U}\right) \frac{a^2}{2[\overline{X^2}]} \cdot \exp\left\{-\frac{r^2}{2\overline{X^2}}\right\} \qquad (31)$$

$$\frac{C}{C_A} = \left(\frac{U_{AVG}}{U}\right) \sum_0^\infty \exp\left\{-\frac{\beta_n^2}{2}\overline{X^2}\right\} \cdot \frac{J_0(r\beta_n)}{J_0^2(a\beta_n)} \qquad (32)$$

The term U_{AVG}/U is the ratio of the average fluid velocity in the bed to the velocity of the diffusing material. Thus if the field were such that the fluid velocity were larger in the center than in other portions and if diffusion measurements were made only in this region then (U_{AVG}/U) would be less than unity. The parameter U_{AVG}/U can be evaluated directly from a concentration profile for cases in which longitudinal diffusion is negligible through the relation

$$U_{AVG}/U = \overline{C/C_A} \qquad (33)$$

The validity of this equation can be proved by considering the case in which C/C_A is negligible at the wall:

$$\overline{C/C_A} = \int_0^a \frac{(C/C_A)\, d(r^2)}{a^2}$$

Substituting from Equation (31) for C/C_A gives

$$\overline{C/C_A} = \frac{\left(\frac{U_{AVG}}{U}\right) \frac{a^2}{2[\overline{X^2}]} \int_0^a \exp\left\{-\frac{r^2}{2\overline{X^2}}\right\} d(r^2)}{a^2}$$

Since C/C_A is negligible at the wall

$$\left(\frac{U_{AVG}}{U}\right) \frac{a^2}{2\overline{X^2}} \exp\left\{-\frac{r^2}{\overline{X^2}}\right\} \to 0$$

integration of the equation for $\overline{C/C_A}$ results in Equation (33).

Relations for center-line concentrations can be obtained from Equations (31) and (32) by setting $r = 0$:

wall reflections unimportant:

$$(C/C_A)_0 = \left(\frac{U_{AVG}}{U}\right) \frac{a^2}{2\overline{X^2}} \qquad (34)$$

wall reflections important:

$$(C/C_A)_0 = \left(\frac{U_{AVG}}{U}\right) \sum_0^\infty \frac{1}{J_0^2(a\beta_n)} \cdot \exp\left\{-\frac{\beta_n^2}{2}\overline{X^2}\right\} \qquad (35)$$

Therefore, for cases in which U_{AVG}/U is known, $\overline{X^2}$ may be obtained as a function of z from center-line traverses provided Equations (31) and (32) are valid in describing radial-concentration profiles. This is shown to be true for distances far from the source. Close to the source Equation (31) does not describe the entire profile, owing to longitudinal diffusion. However, the effects of longitudinal diffusion are confined to the outer regions and Equation (31) may still be used to calculate the center-line concentrations. Frenkiel (5) has calculated concentration profiles for the asymptotic case of $t \to 0$ and $R(s) \to 1$. These show

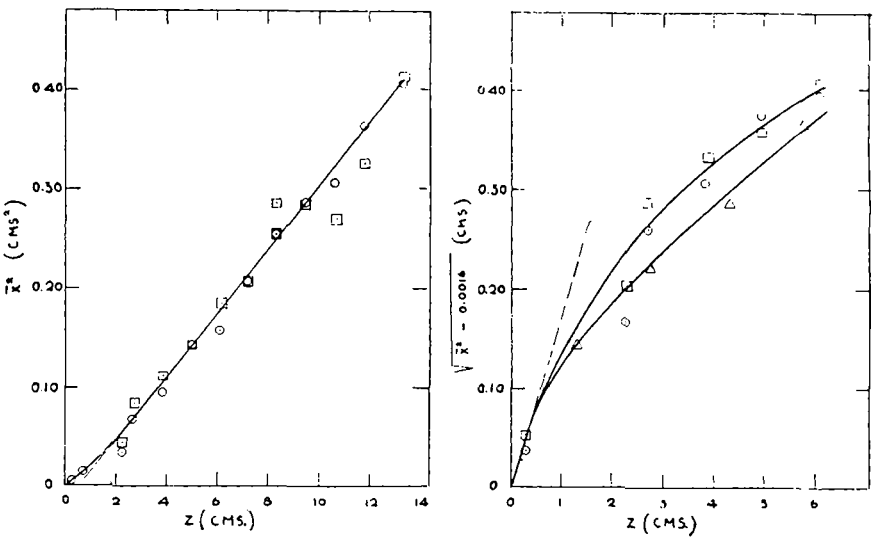

Fig. 6. Empty-tube data. $\overline{X^2}$ vs. z and $\sqrt{\overline{X^2} - 0.0016}$ vs. z.

that for small intensities, $\sqrt{\overline{u^2}}/U$, Equation (31) is valid. As the intensity approaches a value of about 0.1, however, the concentration profile digresses from the Gaussian distribution at large values of r. As the intensity increases, this effect extends itself to smaller r. However, the concentration at $r = 0$ is not affected until the intensity reaches a value larger than 0.5.

The relation between $\overline{X^2}$ and $(C/C_A)_0$ as calculated from Equations (34) and (35) for the case of $U_{AVG}/U = 1$ are presented in Figure 5. It can be seen from this graph that reflections of tracer substance from the wall do not affect these calculations until C/C_A at the tube center drops to a value of about 2.2. Values of $\overline{X^2}$ obtained from this graph are not the actual mean square displacement of the material at the level under consideration but are values describing the spread under the hypothetical condition of no confining walls and mean velocity of zero. The mean square displacement so computed may be used directly to secure turbulence parameters of interest.

Limiting Value of E

With Equations (5) and (24), corrected for flow, applied to the limiting slope of $\overline{X^2}$ vs. z at large values of z, the slope is shown to be the limiting value of E/U. Since this equals $U\tau(\sqrt{\overline{u^2}}/U)^2$, evaluation of the scale τ or the intensity $\sqrt{\overline{u^2}}/U$ will completely define the system, provided that U of the tracer is the same as the mixed average fluid velocity, i.e., $U = U_{AVG}$, or that U/U_{AVG} is known.

Intensity, $\sqrt{\overline{u^2}}/U$

Application of Equation (3) in a flow system to the initial slope of an $\sqrt{\overline{X^2}}$ vs. t curve results in a slope with a numerical value of the intensity. Extraction of turbulence intensity by this route presents difficulties because (1) the source is finite and therefore at $z = 0$, $\overline{X^2} \neq 0$ and (2) it is not possible to make measurements very close to the source without altering the system between the injector and sampling probe.

In order to estimate the effect of the initial displacement of tracer due to the finite source, the data were treated in the relationship $\sqrt{\overline{X^2} - \overline{X_0^2}}$ vs. z. $\overline{X_0^2}$ is the initial displacement at the source, which may be derived as follows:

$$\overline{R_0^2} = \overline{X_0^2} + \overline{Y_0^2} = 2\overline{X_0^2}$$

$$\overline{R_0^2} = \frac{\int_0^b r^2 2\pi r\, dr}{\pi b^2} = \frac{b^2}{2}$$

$$\overline{X_0^2} = \frac{b^2}{4}$$

For the tracer tube used, $\overline{X_0^2}$ has a value of 0.0016 sq. cm.

The variable $\sqrt{\overline{X^2} - \overline{X_0^2}}$ should extra-

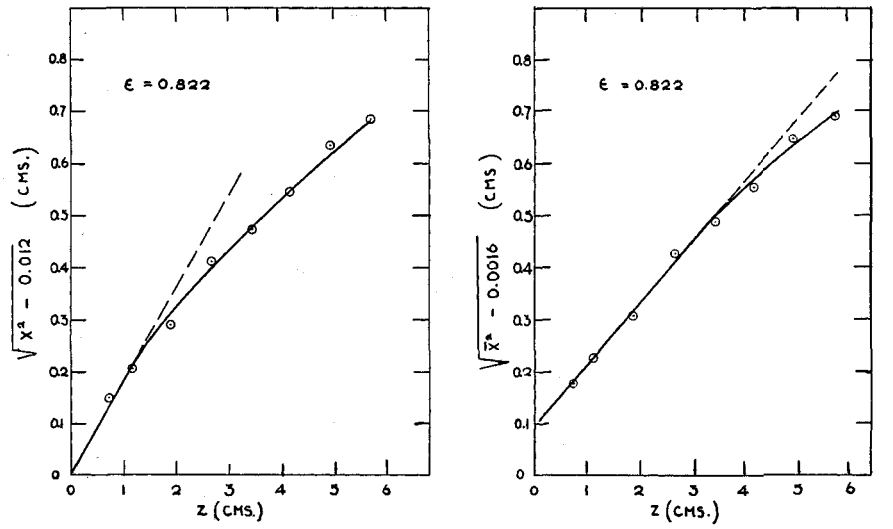

Fig. 7. Typical fluidized-bed data showing the effect of selecting values for X_0^2 in the ordinate, $\sqrt{\overline{X^2} - \overline{X_0^2}}$.

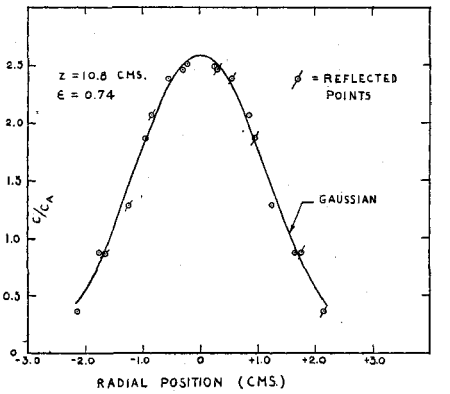

Fig. 8. Typical Gaussian distribution of tracer substance in particulately fluidized bed at substantial distance from source.

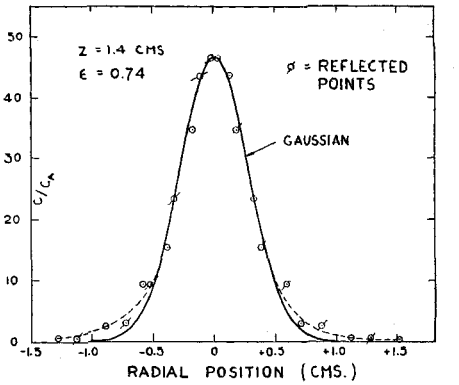

Fig. 9. Typical distribution of tracer substance in a particulately fluidized bed at a level close to the source, showing deviation from a Gaussian distribution at the larger radial positions.

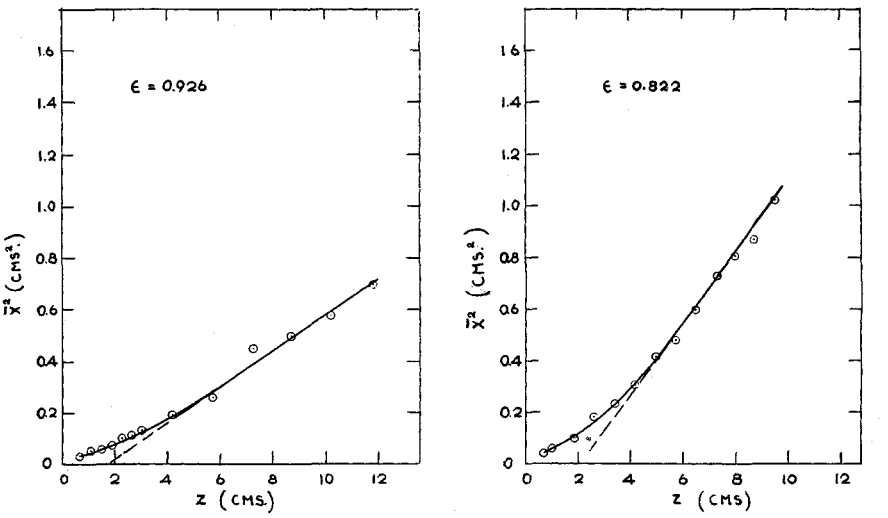

Fig. 10. Typical $\overline{X^2}$ vs. z curves obtained from axial traverses of tracer composition.

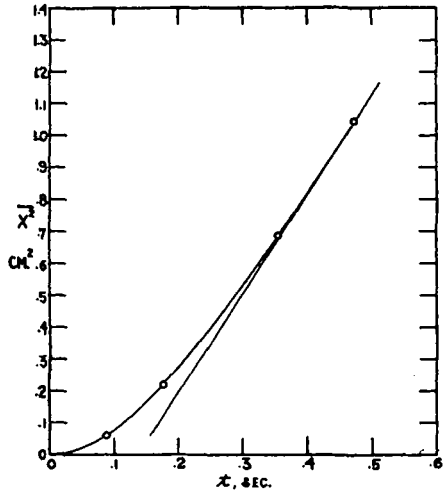

Fig. 11. $\overline{X^2}$ vs. t for 3.4-mm. glass beads fluidized in water at $\epsilon = 0.80$; experimental points determined by full radial traverses at different z positions.

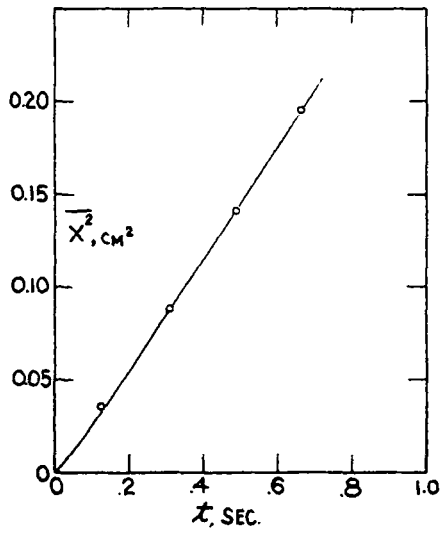

Fig. 12. $\overline{X^2}$ vs. t for 1.8-mm. glass beads fluidized in water at $\epsilon = 0.90$; experimental points determined through full radial traverses at different z positions.

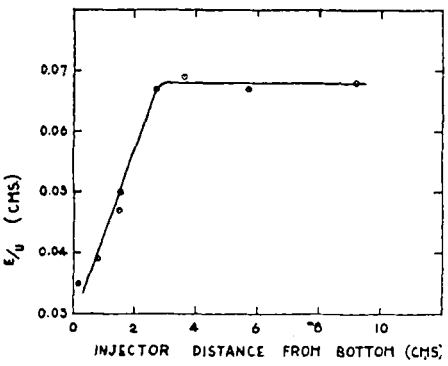

Fig. 13. Asymptotic values of E/U related to the distance of the tracer injector from the grid-bed support.

polate to a value of zero at $z = 0$ as a gross test of the relationship. Data from empty-tube measurements (Figure 6) conform quite well when $\overline{X_0^2}$ is taken at the aforementioned value. However, in the case of all fluidization runs with glass spheres the value of $\overline{X_0^2}$ had to be adjusted to an empirical value of 0.012 sq. cm. This single value sufficed for all fluidization experiments (Figure 7). It would appear that the effective diameter of the injector during fluidization is approximately three times the internal diameter of the tube. It is possible that collisions of particles with the injector tip serve to spread the emerging dye stream.

Scale, τ

The most convenient route to the scale is first to assume the function $R(s) = \exp(-s/\tau)$, which validates Equation (9). When this equation for the limiting asymptote of the $\overline{X^2}$ vs. t curve is rewritten in the form below,

$$\overline{X^2} = \frac{2\overline{u^2}\tau z}{U} - 2\overline{u^2}\tau^2 \qquad (36)$$

it can be seen that the scale τ can be evaluated from the intercept on the z axis, z_0.

$$z_0 = U\tau \qquad (37)$$

A judgment of the validity of the assumptions may be achieved through comparison of the complete experimental $\overline{X^2}$ vs. curve, especially in the curvilinear section, with the same complete function [Equation (10)] computed from the assumed relation for R. An alternative procedure to evaluate τ(*9, 14, 15*) involves double differentiation of $\overline{X^2}$ vs. t data in the nonlinear section, where $R > 0$. Because of questionable precision, this latter method was not chosen in the present work.

RESULTS

Experiments were conducted over the gross linear velocity range from 4 to 26 cm./sec. encompassing fractions void between 0.47 and 0.93.

Typical radial-concentration profiles are shown in Figures 8 and 9. Individual experimental points are used twice, as original points and as reflected points on the other lobe of the curve. At substantial distances from the source (Figure 8) diffusion is described by a Gaussian type of curve [Equation (31)]. However, close to the source, as in Figure 9, profiles diverge from a Gaussian distribution at large values of r, probably because of longitudinal diffusion. Application of Equation (26) gives a similar divergence. As shown in Figure 9, however, the data diverge much more than would be predicted by Equation (26). This could be due to nonhomogeneities in the field caused by the presence of the injector or to the nonisotropic nature of the field. Equation (26) assumes that diffusion in the direction of mean flow is the same as in the radial direction. This assumption, as was pointed out in the theory section, is probably not true. A similar divergence between experimental and predicted results on the basis of a homogeneous isotropic field was obtained by Hinze and van der Hegge (7) on the spread of heat in a gas stream close to the source.

Values of U_{AVG}/U were determined through the use of Equation (33) applied to radial-concentration profiles. The results, presented in Table 1, indicate that

Table 1. Summary of U_{AVG}/U Values from Radial Traverses

$\frac{U_{AVG}}{U}$	U, cm./sec.	ϵ	z, cm.
1.0	16.0	0.737	1.4
1.0	16.0	0.737	1.9
0.7	16.0	0.737	0.95
1.0	16.0	0.737	10.8
0.7	16.9	0.816	1.5
0.8	16.9	0.816	3.0
1.1	16.9	0.816	6.0
1.0	16.9	0.816	8.0
0.9	23.6	0.914	1.4

$U_{AVG}/U \approx 1$ at all levels in the tube. Fluid velocity is apparently quite uniformly distributed in the tube. It should be noted that calculation of the ratio is highly sensitive to a displacement of the center of the concentration traverse from the center of the tube.

$\overline{X^2}$ vs. z curves were determined, in the main, from center-line traverses, a typical set being illustrated in Figure 10. Figures 11 and 12 present similar data, but plotted against time rather than distance. This particular pair of curves was determined from full radial traverses at each z level, Figure 11 being for fluidization of 3.4-mm. glass beads and Figure 12 for 1.8-mm. beads, the former being at a void fraction of 0.80 and the latter, 0.90. Notable was the high visual uniformity of the bed with the smaller particles and the relatively small $\overline{X^2}$ and scale as indicated in Figure 12.

End effects are depicted in Figure 13, which presents asymptotic values of E/U (at large spacings between injector and sampling tubes) as a function of the distance of the injector from the bottom grid plate. A uniform field is not obtained until the injector is placed about 2.5 cm. from the support plate. In all axial traverses, therefore, the injector was placed at the safe distance of 4.6 cm. from the bottom. Taking traverse data in the upper few centimeters of the fluidized bed was also avoided.

All $\overline{X^2}$ vs. z results in this work are correlated in Figure 14 by the dimensionless variables $\overline{X^2}/2(E/U)_{1.0}z_0$ and z/z_0. These variables are derived by a combination of Equations (9), (10), and (24). Clearly, the type of relation predicted by

Taylor for homogeneous, isotropic turbulence is achieved in a particulately fluidized bed.

A comparison is afforded in Figure 15 to show the closely similar characteristics of turbulence in the present water-fluidized beds and turbulence as measured in an open channel by Kalinske and Pien (*9*). The "calculated curve" is computed by means of Equation (10) and represents the form of the correlation function R as given in Equation (6). It appears that this function may be considered only as a convenient first approximation to a correlation function that completely expresses fluid-bed turbulence properties.

Turbulence intensities were computed from center-line traverses by two alternate methods. The first method involved determination of the time scale τ through the intercept of $\overline{X^2}$ vs. z curves and computation of $\sqrt{\overline{u^2}}/U$ from Equations (36), (13), and (17) as discussed under Reduction of Data. The second method secured the intensity from the initial slope of a $\sqrt{\overline{X^2} - \overline{X_0^2}}$ vs. z plot. Figure 7 gives a typical plot of the latter function and illustrates the effect of choosing different values of $\overline{X_0^2}$, the value of 0.0016 stemming directly from the dimensions of the injector tip, the value of 0.012 being an empirically chosen value such that the function passes through the origin. Table 2 presents a comparison of intensities computed by the two methods. The agreement between the two is considered satisfactory.

FLUID-BED PROPERTIES

The mixing properties of a fluidized bed are observed to vary in an interesting manner as, with increasing fluid velocity, the particle population is varied over the full possible range, from a fixed bed to a tube containing no particles. The mixing properties include the Peclet number, $D_p U/(E_{1.v.})$, turbulence intensity, $\sqrt{\overline{u^2}}/U$, a measure of the life of a turbulent eddy, τ, and a length, l, representing the scale of turbulence. The latter variable is defined through the equation

$$E_{1.v.} = l\sqrt{\overline{u^2}} \qquad (38)$$

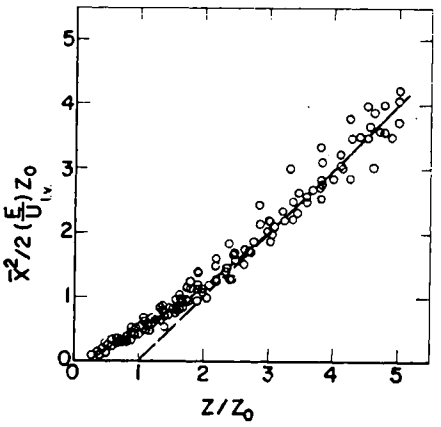

Fig. 14. Generalized plot of all 3-mm. glass-bead fluidization data, $\overline{X^2}/2(E/U)z_0$ vs. z/z_0.

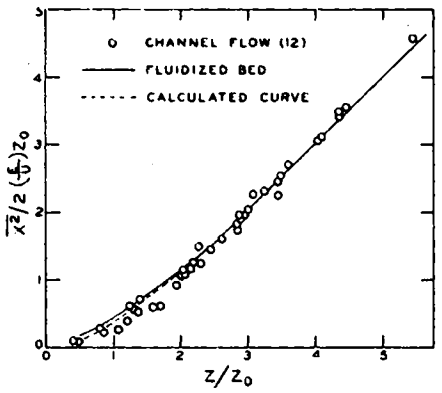

Fig. 15. Generalized plot of fluidization and channel-flow turbulent spreading of tracer substance. A calculated curve also is presented, based upon the form of the correlation function, $R(s) = \exp(-s/\tau)$.

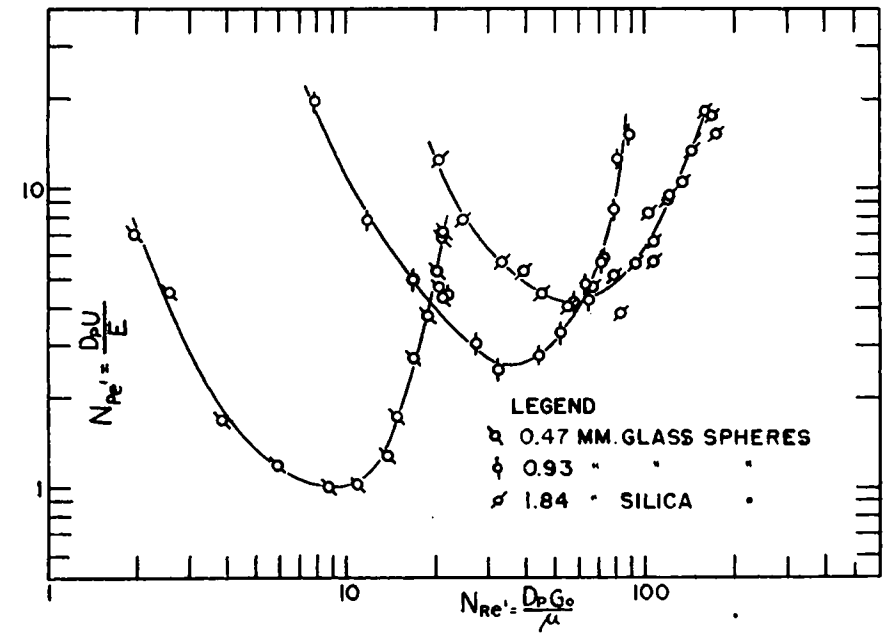

Fig. 16. Variation of Peclet number with Reynolds number during the fluidization in water of three different sizes of particles.

Table 2. Comparison of Turbulence Intensities Calculated by Intercept of $\overline{X^2}$ vs. z Curve and by the Initial Slope of the $\sqrt{\overline{X^2} - \overline{X_0^2}}$ vs. z Curve $\sqrt{\overline{u^2}/U}$

ϵ	Intercept	Initial slope
0.93	0.14	0.16
0.90	0.15	0.15
0.89	0.16	0.17
0.88	0.16	0.17
0.85	0.16	0.15
0.77	0.19	0.18
0.74	0.20	0.19
0.71	0.19	0.18
0.69	0.23	0.18
0.65	0.24	0.25
0.61	0.32	0.25
0.57	0.28	0.22
0.54	0.23	0.21
0.47	0.30	0.23
0.82	0.17	0.19
0.82	0.19	0.21
0.82	0.16	0.19
0.82	0.18	0.18

PECLET NUMBER DURING FLUIDIZATION

The change of the Peclet group during fluidization as fluid velocity (Reynolds number) is increased and as the particle population simultaneously is decreased is shown in Figure 16 for three different sizes of particles. A minimum Peclet number (maximum E) is found for each particle size to correspond to a fraction void of about 0.70. Mixing in a packed bed was found (*12*) to be explainable in terms of a random-walk model, and it is suggested that a dense fluidized bed retains elements of this mechanism. The distance a fluid element must side step in order to pass around a particle increases as the bed is expanded. Eventually, at a fraction void of 0.70, a fluid element may begin to flow past solid particles without the necessity at each level of flowing laterally in order to evade a particle. Beyond the critical fraction void, in dilute beds, the turbulence is particle generated and the eddy diffusivity then is a direct function of particle population, leading to an increase in Pe as Re is increased (and the population is thereby decreased between the tracer source and sample probe).

The manner in which the limits of a fluid bed are approached in the case of 3-mm. beads when the Peclet number is

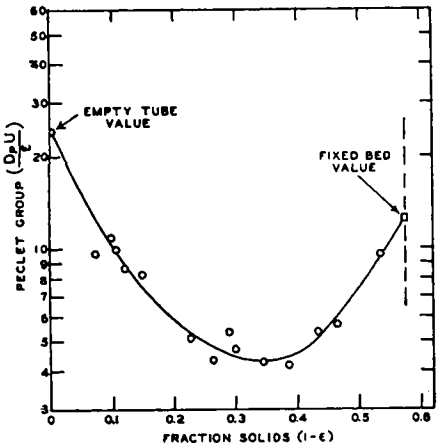

Fig. 17. Peclet-number variation with fraction solids during expansion of fluid bed of 3-mm. particles in water between the limits of an empty tube and a fixed bed.

related to fractions solid is shown in Figure 17. The Peclet number for a fixed bed was determined in a separate tracer-diffusion study (*12*).

SCALE AND INTENSITY

The variation of scale and intensity with fraction solids for a fluidized bed of 3-mm. particles is presented in Figure 18. Consistent with the model presented above for variation of *Pe*, the scale is observed to achieve a maximum value at a fraction void of about 0.70. The intensity is noted to vary directly with particle population although there are uncertainties at the limits. Fixed-bed values for scale and intensity were estimated through a calculation based upon the random-walk model (*5*).

NOTATION

a = fluid-bed radius
b = tracer-tube internal radius
C = concentration of diffusing material
C_A = mixed average concentration in column effluent
D_p = particle diameter
D_t = tube diameter
E = eddy diffusion coefficient = $\overline{X^2}/2t$
$E_{l.v.}$ = limiting value of eddy diffusion coefficient
$J_0(\ )$ = Bessel function of first kind, zero order
Q = source strength
r = radial distance
Re = Reynolds number
R_0 = correlation coefficient

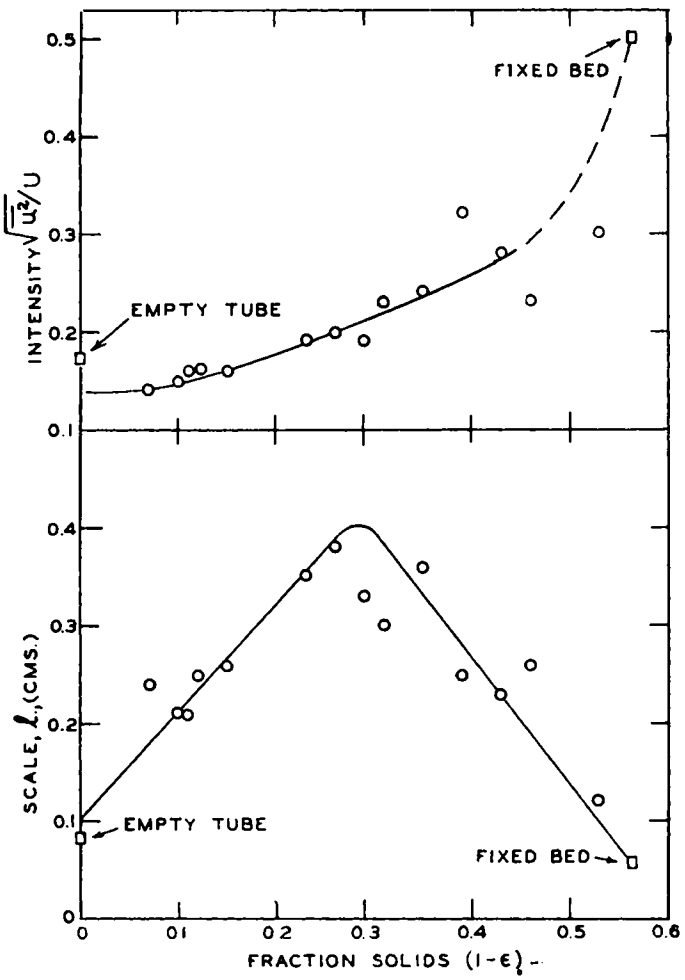

Fig. 18. Scale and intensity of turbulence in water-fluidized bed of 3-mm. glass spheres as function of fraction solids; empty-tube values by experiment, fixed-bed values through calculation based on random-walk model.

$$\frac{\overline{u_{t1}u_{t2}}}{\sqrt{\overline{u^2}_{t1}}\sqrt{\overline{u^2}_{t2}}}$$

S = $x^2 + y^2 + z^2$
s = increment of time = $t_2 - t_1$
t = time
U = fluid velocity associated with tracer material within fluidized bed
U_{AVG} = average velocity over the tube cross section within fluidized bed
u = velocity component in x direction
v = velocity component in y direction
w = velocity component in z direction
X = displacement in x direction
x = distance along x coordinate
y = distance along y coordinate
z = distance in the direction of flow
z_0 = intercept of $\overline{X^2}$ vs. z limiting slope on z axis
ϵ = fractions void
$(\beta_n a)$ = positive roots of Bessel function of first kind, first order. Dividing roots by a gives values of β_n.
τ = constant characteristic of a particular turbulent system

LITERATURE CITED

1. Batchelor, G. K., *Australian J. Sci. Research*, **A2**, 437 (1949).
2. Bernard, R. A., and R. H. Wilhelm, *Chem. Eng. Progr.*, **46**, 233, (1950).
3. Einstein, Albert, *Ann. Physik*, **17**, 549 (1905); **19**, 371, (1906).
4. Frenkiel, F. N., "Advances in Applied Mechanics," vol. 3, Academic Press, Inc., New York (1953).
5. Hanratty, T. J., Ph.D. thesis, Princeton Univ., Princeton, N. J. (September, 1953).
6. ———, *A.I.Ch.E. Journal*, **2**, 42 (1956).
7. Hinze, J. O., and B. G. van der Hegge Zijnen, paper presented at the Institute of Mechanical Engineers General Discussion on Heat Transfer, London (September, 1951).
8. Kalinske, A. A., and E. R. Van Driest, "Fifth International Congress for Applied Mechanics," John Wiley and Sons, New York (1938).
9. Kalinske, A. A., and C. L. Pien, *Ind. Eng. Chem.*, **36**, 220 (1944).
10. Kampe de Feriet, *Ann. Soc. Sci. Bruxelles*, **159**, 145 (1939).
11. Klinkenberg, Adriaan, R. J. Krajenbrink, and H. A. Lauwerier, *Ind. Eng. Chem.*, **45**, 1202 (1953).
12. Latinen, G. A., Ph.D. thesis, Princeton Univ., Princeton, N. J., (December, 1951).
13. Schubauer, G. B., *Natl. Advisory Comm. Aeronaut., Rept.* 524 (1935).
14. Taylor, G. I., *Proc. London Math. Soc.*, **20A**, 196 (1921).
15. ———, *Proc. Roy. Soc. (London)*, **151A**, 421 (1935).
16. Towle, W. L., T. K. Sherwood, and L. A. Seder, *Ind. Eng. Chem.*, **31**, 457 (1939).
17. Townsend, A. A., *Proc. Cambridge Phil. Soc.*, **A43**, 560 (1947).
18. ———, *Proc. Roy. Soc. (London)*, **A209**, 418 (1951); **A224**, 487 (1954).
19. Uberoi, M. S., and Stanley Corrsin, *Natl. Advisory Comm. Aeronaut. Rept.* 1142 (1953).